XBP1s Links the Unfolded Protein Response to the Molecular Architecture of Mature N-Glycans

Citation: Dewal, Mahender B. et al. "XBP1s Links the Unfolded Protein Response to the Molecular Architecture of Mature N-Glycans." Chemistry & Biology 22.10 (2015): 1301–1312.

As Published: http://dx.doi.org/10.1016/j.chembiol.2015.09.006

Publisher: Elsevier

Persistent URL: http://hdl.handle.net/1721.1/106600

Version: Author's final manuscript: final author's manuscript post peer review, without publisher's formatting or copy editing

HHS Public Access

Author manuscript

Chem Biol. Author manuscript; available in PMC 2016 October 22.

Published in final edited form as:

Chem Biol. 2015 October 22; 22(10): 1301–1312. doi:10.1016/j.chembiol.2015.09.006.

XBP1s Links the Unfolded Protein Response to the Molecular Architecture of Mature N-Glycans

Mahender B. Dewal[1], **Andrew S. DiChiara**[1], **Aristotelis Antonopoulos**[2], **Rebecca J. Taylor**[1], **Chyleigh J. Harmon**[1], **Stuart M. Haslam**[2], **Anne Dell**[2], and **Matthew D. Shoulders**[1,*]

[1]Department of Chemistry, Massachusetts Institute of Technology, Cambridge, MA 02139, USA

[2]Department of Life Sciences, Imperial College London, London SW7 2AZ, United Kingdom

SUMMARY

The molecular architecture of the mature N-glycome is dynamic, with consequences for both normal and pathologic processes. Elucidating cellular mechanisms that modulate the N-linked glycome is, therefore, crucial. The unfolded protein response (UPR) is classically responsible for maintaining proteostasis in the secretory pathway by defining levels of chaperones and quality control proteins. Here, we employ chemical biology methods for UPR regulation to show that stress-independent activation of the UPR's XBP1s transcription factor also induces a panel of N-glycan maturation-related enzymes. The downstream consequence is a distinctive shift towards specific hybrid and complex N-glycans on N-glycoproteins produced from XBP1s-activated cells, which we characterize by mass spectrometry. Pulse-chase studies attribute this shift specifically to altered N-glycan processing, rather than to changes in degradation or secretion rates. Our findings implicate XBP1s in a new role for N-glycoprotein biosynthesis, unveiling an important link between intracellular stress responses and the molecular architecture of extracellular N-glycoproteins.

INTRODUCTION

The endoplasmic reticulum (ER) is a specialized protein folding factory responsible for producing about one-third of the proteome (Braakman and Bulleid, 2011). The vast majority of proteins traversing the ER are co- or post-translationally N-glycosylated by oligosaccharyl transferase (OST) (Aebi, 2013; Zielinska et al., 2010). A 14-residue oligosaccharide with the structure $Glc_3Man_9GlcNAc_2$ is transferred by OST from the lipid-linked precursor $Glc_3Man_9GlcNAc_2$-pyrophosphate-dolichol to the amide nitrogen of Asn sidechains in Asn-Xaa-Ser/Thr sequons (where Xaa ≠ Pro). This immature N-linked glycan

*Corresponding Author: Matthew D. Shoulders, Department of Chemistry, Massachusetts Institute of Technology, 77 Massachusetts Avenue, 16-573A, Cambridge, MA 02139, Phone: (617) 452-3525, Facsimile: (617) 324-0505, mshoulde@mit.edu.

SUPPLEMENTAL INFORMATION

Supplemental Information including Supplemental Experimental Procedures, two tables, and four figures can be found with this article online.

is later processed and modified in both the ER and the Golgi to ultimately yield the vast array of distinct molecular structures observed on mature ER clients (Moremen et al., 2012).

Protein N-glycosylation has important implications for numerous normal and pathologic processes (Dennis et al., 2009), including protein folding and stability (Chen et al., 2010; Culyba et al., 2011), function (Venetz et al., 2015), trafficking (Wujek et al., 2004), quality control (Ruiz-Canada et al., 2009), and aggregation (Ioannou et al., 1998), as well as auto-immunity and tumor metastasis (Chui et al., 2001; Hauselmann and Borsig, 2014). Furthermore, although the architecture of the highly diverse, mature N-linked glycome is known to be dynamic, responding to environmental conditions and other stimuli (Hassinen et al., 2011; Lau et al., 2007), the upstream cellular mechanisms that regulate the composition of the N-glycome remain poorly delineated (Voss et al., 2014). Elucidating those mechanisms is important not just for understanding normal and disease physiology, but also for optimizing the production of recombinant proteins displaying desirable N-glycoform populations (Elliott et al., 2003).

The composition of the secretory pathway's proteostasis network, which is responsible for the folding and quality control of secreted, transmembrane and lysosomal proteins, including all N-glycoproteins, is regulated by the unfolded protein response (UPR) (Ron and Walter, 2007). The UPR typically activates in response to ER stress caused by the accumulation of unfolded and misfolded proteins. Aside from transient inhibition of new protein synthesis, the crucial consequence of this stress-responsive UPR activation is a large-scale remodeling of the ER proteostasis network via transcriptional upregulation of chaperones, folding enzymes, and quality control factors. These transcriptional responses are propagated by two UPR-specific transcription factors, X-box binding protein 1-spliced (XBP1s) and activating transcription factor 6 (ATF6), as well as a third transcription factor, ATF4, that can also be induced by independent stress response pathways (Schroder and Kaufman, 2005). UPR-mediated upregulation of chaperones and quality control mechanisms can restore ER proteostasis in response to a variety of protein misfolding-inducing stressors.

A classic method to activate the UPR and thereby study its function is the inhibition of ER client protein N-glycosylation by treatment with tunicamycin (Tm), which prevents the synthesis of the dolichol-linked N-glycan precursor (Lehle and Tanner, 1976), highlighting the importance of N-glycosylation for ER proteostasis. The absence of N-linked glycans on nascent ER clients prevents access to the key ER lectin-based chaperones calnexin and calreticulin, restricts monitoring by the lectin-based quality control machinery, and can also intrinsically destabilize ER clients (Hammond et al., 1994).

Thus, the paradigmatic role of the UPR is to up-regulate chaperones and quality control mechanisms in response to protein misfolding stress. Because N-glycosylation sequons are normally only partially occupied (Zielinska et al., 2010), it is reasonable to also expect that UPR activation might enhance the extent of ER client protein N-glycosylation (Hammond et al., 1994; Spear and Ng, 2005; Thibault et al., 2011). Such an enhancement would specifically increase access to lectin-based proteostasis mechanisms. Consistent with this concept, ER stress can upregulate hexosamine biosynthesis to promote ER client clearance

and prolong life in the face of chronic protein misfolding stress (Denzel et al., 2014; Wang et al., 2014).

We speculated that the UPR might regulate not just the extent of protein N-glycosylation, but also the molecular structure of mature N-glycans. Mature N-glycan architectures are substantially altered in many malignancies (Fry et al., 2011; Hauselmann and Borsig, 2014; Stowell et al., 2015), yet the mechanisms that regulate these altered N-glycosylation patterns remain ill-defined. Concomitantly, it is intriguing to note that a number of malignancies appear to rely on the activation of pro-survival pathways within the UPR, including constitutive activation of the XBP1s transcription factor (Bagratuni et al., 2010; Carrasco et al., 2007; Fujimoto et al., 2003). These observations, in addition to the overarching role of the UPR in regulating ER client protein folding and trafficking, suggested to us that there may be a connection between UPR activity and N-glycan maturation patterns.

Testing our hypothesis requires studying the biosynthesis of N-glycoproteins in the presence or absence of UPR-mediated remodeling of the ER proteostasis network. Unfortunately, ER stress-inducing small molecules like Tm, thapsigargin, or dithiothreitol activate the UPR by creating non-physiologic levels of protein misfolding stress and are highly cytotoxic. These undesired side effects convolute efforts to study the roles of UPR activation and the resultant ER proteostasis network remodeling in protein maturation.

To overcome this challenge, small molecule-regulated methods for the orthogonal, stress-independent activation of the key adaptive UPR transcription factors XBP1s and ATF6 in human cells have been pioneered (Lee et al., 2003; Shoulders et al., 2013b). Specifically, the ATF6 transcription factor can be regulated by fusion to a DHFR destabilized domain that is stabilized by administration of trimethoprim (TMP) (Iwamoto et al., 2010; Shoulders et al., 2013a), while XBP1s can be placed under control of the tetracycline repressor and activated by doxycycline (Dox). In cells carrying these chemical genetic tools, such as the HEK293^{DAX} cell line (Shoulders et al., 2013b), the functional consequences of physiologically relevant, UPR transcription factor-mediated remodeling of the ER proteostasis network can be studied in the absence of toxic protein misfolding stress created by molecules like Tm, thapsigargin, or dithiothreitol.

Here, we employ stress-independent UPR activation to elucidate whether and how UPR-mediated remodeling of the ER proteostasis network regulates N-glycan maturation. We demonstrate that the XBP1s transcription factor is responsible for modulating N-glycan maturation on model secreted proteins, resulting in enhanced synthesis of both hybrid and complex N-glycans. Cumulatively, our results unveil the capacity of the IRE1-XBP1s axis of the UPR to modify N-glycan maturation, unveiling a previously unknown link between intracellular proteostasis mechanisms and the molecular architecture of extracellular N-glycoproteins.

RESULTS

Transcriptional Regulation of N-Glycan Biosynthesis and Maturation Pathways by the Unfolded Protein Response

Affymetrix whole genome arrays were previously used to evaluate the transcriptome of HEK293^{DAX} cells upon small molecule-mediated activation of XBP1s and/or ATF6 (Shoulders et al., 2013b). It was observed that these transcription factors control the levels of partially overlapping sets of ER chaperoning and quality control mechanisms. Interestingly, gene ontology enrichment analysis shows that five of the top 24 and two of the top 10 gene sets induced by XBP1s are related to N-glycosylation of ER clients (Shoulders et al., 2013b). Of particular note, numerous components of the N-glycoprotein biosynthesis machinery are upregulated by XBP1s or the combination of XBP1s and ATF6 activation (see Table S1 for quantitative data), including components of the oligosaccharyltransferase complex and enzymes involved in the synthesis of the dolichol-linked precursor to N-glycosylation (Figure 1A; regular italic typeface).

Considering the essential roles of N-glycans in providing access to the ER proteostasis network (Hammond et al., 1994), it is unsurprising to observe that enzymes involved in the extent to which ER clients are N-glycosylated are upregulated by the UPR transcription factors. Intriguingly, we also observe numerous enzymes likely involved in N-glycan maturation that are upregulated by XBP1s or the combination of both XBP1s and ATF6 (Figure 1A; bold italic typeface) (Shoulders et al., 2013b). The possible connection to ER proteostasis is arguably less apparent for these enzymes than for those involved in initial N-glycoprotein biosynthesis. However, the UPR plays a critical role not just in protein folding, but also in ER client trafficking and propagating intracellular stress signals to the extracellular milieu (Taylor and Dillin, 2013). Therefore, motivated by these transcript-level results, we proceeded to explore the possible functional consequences of XBP1s and/or ATF6 activation for the maturation of N-glycans installed on ER client proteins.

XBP1s Modulates N-Glycan Maturation on a Secreted N-Glycoprotein

We elected to employ the CD2 adhesion domain, a well-characterized ER client protein (Culyba et al., 2011), in our initial studies. The *R. norvegicus* CD2 variant employed, henceforth termed CD2, has the sequence $K_{61}I_{62}F_{63}A_{64}N_{65}G_{66}T_{67}$ at its single N-glycosylation sequon, an N-terminal preprotrypsin signal sequence, a hexa-histidine tag for purification, and a FLAG tag for immunoblotting and immunoisolation (Figure 1B) (Murray et al., 2015). CD2 secreted from HEK293 cells displays two distinctive N-linked glycoform populations that are readily separated by SDS-PAGE analysis (Figure 1C). We confirmed that the two bands observed by immunoblotting of secreted CD2 (N-glycoforms A indicated by the black arrow and N-glycoforms B by the gray arrow in Figure 1C) separate based on their distinctive N-glycan states by showing that PNGase F digestion collapses both bands into a single, lower molecular weight non-glycosylated band indicated by the white arrow.

To investigate the influence of XBP1s- and/or ATF6-mediated remodeling of the ER proteostasis network on CD2 N-glycan maturation, we used CD2-encoding lentivirus to generate stable, clonal HEK293^{DAX} cells constitutively expressing modest levels of CD2,

which we termed HEK293$^{DAX\text{-}CD2}$ cells. The cells were treated with vehicle, 1 μg/mL Dox to activate XBP1s, 10 μM TMP to activate ATF6, or both Dox and TMP to activate both transcription factors. We confirmed successful activation of XBP1s and/or ATF6 by analysis of chaperones known to be induced by these transcription factors (Figure 1D) (Shoulders et al., 2013b), and ensured that global UPR activation does not occur upon dox or TMP treatment by using qPCR to compare the effects of administering the ER stress-inducing small molecule thapsigargin (Figure S1A).

We next analyzed CD2 N-glycosylation in both the media and lysate samples by immunoblotting. In cell lysates, we observe a single high molecular weight N-glycosylated CD2 band and a low intensity non-N-glycosylated CD2 band. Activation of XBP1s and/or ATF6 has no apparent impact on the intracellular quantity of CD2 or the extent of N-glycosylation (Figure 1D). Intriguingly, XBP1s and/or ATF6 activation do have distinctive impacts on secreted CD2 (Figure 1E). CD2 secreted from untreated cells displays the expected two N-glycoforms in a nearly 1:1 ratio. A reduced quantity of CD2 is secreted upon ATF6 activation, but the ratio of N-glycoforms remains unchanged. The quantity of CD2 secreted upon XBP1s activation is similar to untreated cells. Most interestingly, upon XBP1s activation we observe a nearly complete shift of the CD2 N-glycoform population from N-glycoforms B (gray arrow) to N-glycoforms A (black arrow). Also intriguing, we observe the additive effect of XBP1s and ATF6 activation (B→A N-glycoforms shift and reduced secretion) when XBP1s and ATF6 are activated simultaneously.

Quantitation of the N-glycoform A:B ratio in XBP1s and vehicle-treated samples shows a highly significant, ~700% increase in the relative intensity of N-glycoforms A upon XBP1s activation relative to vehicle (Figure 1F). PNGase F digestion of CD2 secreted from XBP1s-activated and untreated cells confirms that the shift in N-glycoform bands is attributable entirely to altered N-glycosylation, as opposed to other possible post-translational modifications (Figure 1G).

As a control, we analyzed CD2 in the media and lysates of transiently transfected HEK293^{DYG} cells (Shoulders et al., 2013b). In these cells, TMP treatment stabilizes DHFR.YFP and Dox treatment induces eGFP. Analysis of CD2 in the media and lysates of HEK293^{DYG} cells shows no change in the extent of secretion or the N-glycoforms A:B ratio upon Dox and/or TMP treatment (Figures S1B and S1C). Thus, the results we observe in HEK293^{DAX} cells are attributable entirely to UPR transcription factor activation, not to any possible off-target effects of the small molecules employed.

Cumulatively, these results show that XBP1s activation increases the levels of particular secreted CD2 N-glycoforms, while ATF6 activation has no effect on the N-glycoforms but does reduce the extent of CD2 secretion. Because we were specifically interested in effects of the UPR on the molecular architecture of the mature N-glycome, we focused exclusively on CD2 produced from XBP1s-activated cells for further studies.

N-Glycoform Maturation Effects Mediated by XBP1s Activation Are Not Attributable to Altered Degradation or Secretion

The XBP1s–mediated shift in the N-glycoform population of mature, secreted CD2 could be caused by altered biosynthesis of the mature N-glycan in the Golgi. A more trivial explanation is that, under XBP1s-activated conditions, a particular CD2 N-glycoform is either degraded or secreted at a different rate than in untreated cells. To test the latter hypothesis, we examined CD2's secretion and degradation rates in untreated and XBP1s-activated HEK293$^{DAX\text{-}CD2}$ cells using [^{35}S]-metabolic labelling (Figure 2A). Relative to untreated cells, we found that XBP1s activation has no effect on the extent of CD2 degradation (Figure 2B). CD2 is indeed partially degraded by the proteasome, as shown by lactacystin-mediated proteasomal inhibition, but to a very similar overall extent under both sets of conditions. XBP1s activation may very modestly decrease the net secretion rate of CD2 over the course of 8 h ($p = 0.03$), but lactacystin treatment completely restores secretion to the levels of untreated cells (Figure 2C). Most importantly, at any time point in the pulse chase experiment, and with or without proteasome inhibition, we observe the identical shift in the CD2 N-glycoforms ratio upon XBP1s activation (Figure 2D). Altogether, these results show that the XBP1s–mediated effects on the architecture of the CD2 N-glycan cannot be attributed to altered CD2 secretion or degradation upon XBP1s activation.

XBP1s Activation Primarily Favors the Synthesis of Hybrid CD2 N-Glycans

To better understand how XBP1s activation alters N-glycan maturation, we next employed selective endo- and exo-glycosidase digestions to structurally classify the N-glycoforms A and B produced from both untreated and XBP1s-activated HEK293$^{DAX\text{-}CD2}$ cells. As illustrated in Figure 3A, Endo-H cleaves both high mannose and hybrid N-glycans, Endo-F_3 cleaves only complex N-glycans, and the combination of α1–2,3-mannosidase and α1–6-mannosidase cleaves only high-mannose N-glycans (Jacob and Scudder, 1994). We found that Endo-H digests both CD2 N-glycoform bands A and B (at the sensitivity of an immunoblot), regardless of XBP1s activation (Figure 3B, black and gray arrows). This result suggests that the majority of the CD2 N-glycans present are high-mannose or hybrid. Consistent with this observation, Endo-F_3 is unable to digest either CD2 N-glycoform band to an observable extent (Figure 3C). The combination of α1–2,3-mannosidase and α1–6-mannosidase, however, clearly reduces the molecular weight of N-glycoforms B (gray arrow), with no effect on N-glycoforms A (Figure 3D, black arrow). These observations suggest that XBP1s activation primarily enhances the biosynthesis of hybrid N-glycans on CD2.

Small Molecule-Mediated Inhibition of Mannosidases to Elucidate XBP1s-Mediated Effects on N-Glycan Biosynthesis

Following the transfer of the original 14-member dolichol-linked N-glycan onto nascent ER client proteins, subsequent removal of the terminal glucose residues by the ER α-glucosidases I and II allows entry to the calnexin and/or calreticulin chaperone folding cycles (Caramelo and Parodi, 2008; Hammond et al., 1994). After folding, additional glucose and mannose residues are removed to yield high-mannose N-glycans that are then

further digested by the Golgi α1–2-mannosidases (Herscovics, 1999). Only subsequent to these additional mannosidase digestions, which yield various additional forms of high mannose N-glycans, can the N-glycan enter downstream processing into mature hybrid and complex N-glycans.

Our data from enzyme digestions indicate that the CD2 N-glycoforms A band, whose synthesis is strongly enhanced by XBP1s activation, is primarily hybrid. Therefore, we expected that inhibiting the catalytic activity of mannosidase enzymes using kifunensine would eliminate the effects of XBP1s activation by preventing the production of mature high-mannose and hybrid N-glycans (Elbein et al., 1990). Indeed, we find that treatment with kifunensine results in observation of only a single N-glycoform band for secreted CD2 (Figure 4A). Although this new band appears at a similar molecular weight to N-glycoforms band A in untreated cells, it is molecularly distinct. Unlike N-glycoform band A (see Figure 3D), the single new band generated by kifunensine treatment is sensitive to digestion by α1–2,3-mannosidase and α1–6-mannosidase, as observed by the small but highly reproducible shift observable by immunoblotting that is expected for this digestion of a high mannose N-glycoform (Figure 4B). Thus, these data show that the effects of XBP1s activation on N-glycan biosynthesis lie downstream of the ER and Golgi α-mannosidase I enzymes.

Swainsonine inhibits Golgi α-mannosidase-II (Tulsiani et al., 1982), which catalyzes the first required step for complex N-glycan biosynthesis. Consistent with our enzyme digestions (Figure 3), swainsonine treatment has no observable impact on the N-glycoforms shift we detect upon XBP1s activation by immunoblotting (Figures 4C and 4D), suggesting once again that XBP1s is primarily enhancing the production of hybrid N-glycans on secreted CD2. We confirmed that Golgi α-mannosidase II was inhibited at the 10 μg/mL swainsonine concentration employed by demonstrating that this treatment prevents the formation of complex N-glycans on erythropoietin (Figure S2).

Glycomic Analysis of Purified CD2 by MALDI-TOF-MS/MS

The data from our glycosidase digestion and inhibition studies suggest that XBP1s activation primarily increases hybrid N-glycan biosynthesis on CD2, at least at the resolution of a gel-based analysis. To obtain a molecular-level, quantitative view of the effects of XBP1s on N-glycan maturation, we performed structural analysis on the N-glycans released from purified CD2 using MALDI-TOF-MS/MS (Ceroni et al., 2008; Jang-Lee et al., 2006). We first optimized a protocol to obtain hundreds of μg quantities of highly purified secreted CD2 from both untreated and XBP1s-activated HEK293$^{DAX\text{-}CD2}$ cells (see Figure S3A). For the untreated sample, we separately extracted N-glycoforms bands A and B for MALDI-TOF-MS/MS analysis. The N-glycoforms band B in the untreated sample (Figure 5A) is relatively homogeneous, with ~95% of the N-glycans being high-mannose and the ~5% hybrid likely deriving from cross-contamination by the upper band A owing to imperfect separation of the bands on SDS-PAGE. The N-glycoforms band A in the untreated sample is ~78% hybrid and ~9% complex (Figure 5B). After normalizing to the relative intensities of N-glycoforms bands A and B in untreated samples (Figure 1F), these MS results indicate that, in untreated cells, approximately 61% of the CD2 produced displays high-mannose N-glycans, ~35% hybrid, and ~5% complex (Table 1).

XBP1s activation almost entirely eliminates the lower N-glycoforms band B, rendering separate extraction and glycomic analysis of N-glycoforms band B not feasible. Therefore, for analysis of N-glycans on CD2 secreted from XBP1s-activated cells, we simply extracted the entire CD2 region from an SDS-PAGE gel (see Figure S3A). Strikingly, MALDI-TOF-MS/MS analysis shows that <11% of the N-glycans on CD2 produced from XBP1s-activated cells are high-mannose, ~74% are hybrid, and ~16% are complex (Figure 5C and Table 1). Normalizing to the relative intensities of bands A and B for the vehicle-treated sample, these results confirm our prediction from enzyme digestions and small molecule inhibition experiments that XBP1s activation strongly favors the biosynthesis of hybrid N-glycans on CD2.

qPCR analyses show that transcripts encoding MAN1A1 and MGAT1 are upregulated by XBP1s activation (Figure S3B). These two proteins are responsible for trimming mannose residues and transferring the first N-acetylglucosamine onto an N-glycan, two critical biosynthetic steps for formation of hybrid N-glycans, and thus could be involved in the observed XBP1s–mediated shift towards hybrid N-glycans. The higher sensitivity of the MALDI-TOF- MS/MS analysis relative to immunoblotting allows us to also observe the >3-fold enhancement in the synthesis of complex N-glycans upon XBP1s activation, which could be mediated in part by MGAT2, another protein whose transcript levels are upregulated by XBP1s (see qPCR data in Figure S3B). MGAT2 catalyzes an early step in the biosynthesis of complex N-glycans.

We note that a number of N-glycoforms are observed upon XBP1s activation that are simply not present on CD2 secreted from untreated cells (Figure 5). Our MALDI-TOF-MS/MS glycomic analyses additionally provide molecular details regarding the terminal structures of the hybrid and complex N-glycans produced in untreated and XBP1s-activated cells. Of particular note, XBP1s activation shifts the population of terminal N-glycoform epitopes observed. Under untreated conditions, ~76% of the N-glycoforms display either LacdiNAc or Fuc-LacdiNAc terminal epitopes. Upon XBP1s activation, this population drops to ~58%, with a corresponding modest increase in LacNAc, LeX/A, LeY/B, and sialylated (S-LacNAc) terminal epitopes (Table 1).

XBP1s–Mediated Effects on N-Glycan Maturation are Generalizable Beyond CD2 and HEK293 Cells

We wondered whether the effects on N-glycan biosynthesis we observe are CD2-specific, or are present more broadly for other N-glycoproteins. To explore this possibility, we created a construct for the expression and analysis of the collagen-α1(I) C-propeptide domain (Shoulders and Raines, 2009). We selected the collagen-α1(I) C-propeptide to study because, like CD2, this ~35 kDa secreted protein has a single N-glycosylation sequon and displays two N-glycoform bands readily separable by SDS-PAGE upon secretion from HEK293^{DAX} cells. We analyzed HA epitope-tagged collagen-α1(I) C-propeptide samples secreted from untreated and XBP1s-activated samples by immunoblotting. We observe that XBP1s activation once again increases the population of a higher molecular weight N-glycoform band (Figures 6A and S4A), without altering the extent of protein secretion and with minimal effects on intracellular levels of the collagen-α1(I) C-propeptide (Figure 6B).

Interestingly, ATF6 activation again decreases the net secretion of the protein with no apparent effects on N-glycosylation, while the combination of XBP1s and ATF6 activation displays an additive effect similar to the consequences for CD2 (Figure 6A). PNGase digestion confirms that the XBP1s–induced shift is caused by an alteration in the N-glycans, as the banding pattern for collagen-α1(I) C-propeptides secreted from both XBP1s-activated and untreated cells are identical upon PNGase digestion (Figure 6C).

We next queried whether the effects of XBP1s activity on N-glycan maturation are limited to just HEK293 cells. CD2 secreted from transiently transfected Saos-2 osteosarcoma cells is observed as a smear of N-glycoforms concentrated in two bands, as confirmed by PNGase digestion (Figure S4B). We transiently transfected CD2 into Saos-2 osteosarcoma cells, transduced the cells with either a GFP or an XBP1s–encoding adenovirus, and examined the N-glycosylation pattern on secreted CD2 under both conditions. We observe a strong enhancement of higher molecular weight N-glycoforms in cells where XBP1s is expressed (Figure 6D). Together, these data indicate that the striking impacts of XBP1s activation on N-glycan maturation are restricted neither just to the CD2 protein nor just to HEK293 cells.

DISCUSSION

Our results demonstrate the capacity of XBP1s–mediated remodeling of the ER proteostasis environment to enhance the biosynthesis of particular hybrid and complex N-glycans. Although it is not yet possible to conclusively attribute the observed alterations in N-glycan maturation to specific enzymes upregulated by XBP1s in Figure 1A, roles for the upregulation of MGAT1 and MAN1A1 in the enhanced synthesis of hybrid N-glycans and the upregulation of MGAT2 in the enhanced synthesis of complex N-glycans are plausible. We speculate that similar XBP1s–induced effects may apply more broadly across the endogenous N-glycoproteome. In ongoing work, we are performing N-glycoproteome-wide studies on endogenous proteins in the context of small molecule-mediated UPR activation to explore this possibility.

Considering the classical role of the UPR in resolving protein misfolding stress, there is the possibility that XBP1s–mediated changes in N-glycosylation patterns assist ER protein folding either indirectly by orchestrating interactions with ER proteostasis network components or directly by altering folding biophysics. Bearing in mind that the IRE1-XBP1s axis is the only arm of the UPR conserved across all eukaryotes (Walter and Ron, 2011), it is alternatively possible that XBP1s simply plays a critical role in regulating all aspects of ER client production. The effects observed need not be linked directly to resolving protein misfolding stress. In such a scenario, regulating N-glycan maturation is a previously unappreciated, yet nonetheless critical role of XBP1s.

There are diverse potential biological implications of XBP1s–mediated regulation of the molecular architecture of mature N-glycans. For example, specific N-glycan structures have roles in processes including protein sorting to microvesicles (Batista et al., 2011) and cell-cell recognition (Sharon, 2007) that would be influenced by altered N-glycan maturation. Additionally, a number of secreted proteins displaying high-mannose N-glycoforms after Golgi processing are known (de Leoz et al., 2011; Satoh et al., 2007), so a specific shift

away from high-mannose N-glycans upon XBP1s activation could influence protein recognition and uptake via the mannose receptor (East and Isacke, 2002). Altered N-glycosylation upon XBP1s activation could also potentially play a role in trans-cellular communication of ER stress (Taylor and Dillin, 2013), an XBP1s–dependent and important biological process for which the relevant signaling molecule remains to be identified.

Of particular interest is the correlation between unusual N-glycoform populations in many cancers (Fry et al., 2011; Hauselmann and Borsig, 2014; Stowell et al., 2015) and constitutive activation of the IRE1-XBP1s UPR axis in certain malignancies (Bagratuni et al., 2010; Carrasco et al., 2007; Fujimoto et al., 2003). There is the possibility that XBP1s activity mechanistically links neoplastic N-glycosylation patterns to chronic ER protein misfolding stress in cancer. An XBP1s–induced shift towards hybrid and especially certain complex N-glycans could enhance tumor invasiveness (Stowell et al., 2015). Our data in Table 1 also suggest that XBP1s activation may increase sialylation. To date, three mechanisms have been proposed to induce hypersiaylation in cancer (Bull et al., 2014); XBP1s activation may represent a fourth mechanism.

Aside from the intriguing biological implications of our findings, we also note that XBP1s activation has previously been employed to increase the yield of recombinant antibodies and other proteins (Tigges and Fussenegger, 2006). Our findings suggest that controlling XBP1s provides a valuable mechanism to modulate N-glycan biosynthesis on recombinant N-glycoproteins, particularly in cases where undesirable high-mannose N-glycans are abundantly produced.

SIGNIFICANCE

The cellular mechanisms that dynamically regulate the N-glycome remain poorly understood. Here, we leverage chemical biology tools for stress-independent, small molecule-mediated control of the UPR to discover that the UPR can regulate the molecular architecture of mature N-linked glycans via XBP1s–mediated remodeling of N-glycan biosynthesis. Specifically, we show that XBP1s activation strongly enhances the synthesis of particular hybrid and complex N-glycans on model secreted proteins. Detailed glycomic analyses show that the identities of terminal glycan epitopes are also influenced by XBP1s activation. These effects cannot be attributed to altered secretion or degradation of particular N-glycoforms, indicating a genuine alteration of N-glycan maturation. Our results are significant because they provide a mechanistic link between intracellular stress responses classically involved in maintaining proteostasis and the molecular architecture of the extracellular N-glycome. There are numerous plausible biological consequences of this freshly drawn connection. In particular, it is well-established that many malignant cells display both unusual N-glycosylation patterns and constitutive XBP1s activation. There may be a causative relationship between these two observations, a possibility we are currently exploring. Also noteworthy, the trafficking of many proteins is influenced by their N-glycan structures, as are the strengths of interactions between N-glycoproteins and various lectins or cell surface proteins. Via these pathways, XBP1s–mediated effects on N-glycan architectures may play a functional role in processes ranging from cancer metastasis to auto-immunity. Furthermore, trans-cellular communication of stress signals plays an important

role in organism survival in the face of stress, yet the signaling molecule has remained elusive. XBP1s–altered N-glycosylation patterns may play a role. Finally, improved methods are needed to optimize N-glycan architectures on recombinant proteins produce for biotechnology applications. Small molecule-mediated, stress-independent control of XBP1s signaling could prove useful for such a purpose.

EXPERIMENTAL PROCEDURES

Cell Culture, Plasmids, and Transfections

HEK293 cells were cultured in Dulbecco's modified Eagle's medium supplemented with glutamine, penicillin/streptomycin, 10% fetal bovine serum, and appropriate selection agents as previously described (Shoulders et al., 2013b). A stable HEK293$^{DAX\text{-}CD2}$ cell line constitutively expressing the CD2 adhesion domain from *R. norvegicus*, whose primary amino acid sequence is shown in the Supplemental Information, was created by transduction of HEK293^{DAX} cells with CD2-encoding lentivirus (Campeau et al., 2009) and maintained in 1.2 μg/mL puromycin after single colony selection. A stable HEK293^{DAX} cell line expressing the collagen-α1(I) C-propeptide was created by calcium phosphate-mediated co-transfection of the appropriate vector (*vide infra*) with a puromycin linear marker (ClonTech) and selection in 1.2 μg/mL puromycin. Saos-2 cells were cultured in complete DMEM supplemented with 15% heat-inactivated FBS. Transient transfections of eGFP-N3 or CD2.pFLAG-CMV3 were performed using polyethylenimine or X-tremeGENE 9 (Roche).

eGFP-N3 and CD2.pFLAG-CMV3 were generous gifts from Prof. J.W. Kelly (Scripps Research Institute). For lentivirus production, the gene encoding CD2 was transferred to pENTR1A using the BamHI and NotI sites and then shuttled into pLenti.CMV.Puro DEST (Campeau et al., 2009) using LR clonase II-mediated recombination. The C-propeptide domain of *COL1A1* (residues 1218–1464) was PCR-amplified from a *COL1A1*-encoding vector and inserted into the pcDNA3.1 vector downstream of a 5'preprotrypsin signal sequence followed by an HA epitope tag.

Immunoblotting and SDS-PAGE

Proteins were separated by SDS-PAGE using 12% Bis-Tris gels. Immunoblotting was performed as previously described (Shoulders et al., 2013b) and analyzed using a Li-Cor Biosciences Odyssey Imager. Antibodies employed are listed in the Supplemental Information.

Quantitative RT-PCR

The relative mRNA expression levels of target genes were measured using quantitative RT-PCR (see the Supplemental Information for details and Table S2 for a list of primers used).

[^{35}S] Metabolic Labeling Experiments

HEK293$^{DAX\text{-}CD2}$ cells seeded on poly-D-lysine-coated plates were treated with Dox at 1 μg/mL to activate XBP1s for 24 h. Cells were then starved for 1 h in DMEM + 10% FBS lacking Cys and Met. Cells were metabolically labeled in pulse medium containing [^{35}S]-

Cys/Met (MP Biomedicals, ~0.1 mCi/mL final concentration) for 20 min, and then incubated in pre-warmed chase media for the indicated times. Lactacystin (10 μM) was added as indicated at the beginning of the chase period. Media was collected and cells were lysed in a 1% Triton X-100 buffer. CD2 was immunopurified using M2 anti-FLAG agarose beads (Sigma; A2220) and washed with RIPA. Immunoisolates were eluted by boiling in 6X–Laemmli buffer and separated by SDS-PAGE. The gels were then dried, exposed to phosphorimager plates (GE Healthcare), and imaged with a Typhoon imager. Band intensities were quantified in ImageQuant TL.

Enzyme Digestions

PNGase-F, Endo-H, Endo-F_3, α1–2,3-mannosidase, and α1–6-mannosidase enzymes were obtained from NEB. Digestions were performed according to the manufacturer's protocols.

MALDI-TOF-MS/MS Glycomic Analyses

CD2 was purified upon secretion from untreated and XBP1s-activated $HEK293^{DAX\text{-}CD2}$ cells and purified CD2 SDS-gel bands were processed for N-glycan analysis as described in the Supplemental Information. MS and MS/MS data were acquired using a 4800 MALDI-TOF/TOF (Applied Biosystems) mass spectrometer. For the MS/MS, the collision energy was set to 1 kV. Ar was used as the collision gas. The 4700 calibration standard kit, Calmix (Applied Biosystems), was used as the external calibrant for the MS mode of both instruments. Human [Glu1] fibrinopeptide B (Sigma) was used as an external calibrant for the MS/MS mode of the MALDI-TOF/TOF instrument. MS and MS/MS data were processed using Data Explorer 4.9 (Applied Biosystems) following the detailed protocol presented in the Supplemental Information.

Supplementary Material

Refer to Web version on PubMed Central for supplementary material.

ACKNOWLEDGEMENTS

The authors gratefully acknowledge Pyae Hein, Amber Murray, and R. Luke Wiseman for helpful discussion. This work was supported by a Mallinckrodt Foundation Faculty Scholar Award, the NIH/NIAMS (1R03AR067503), a Mizutani Foundation for Glycoscience Innovation Grant, the Singapore-MIT Alliance for Research and Technology, and MIT (all to M.D.S.), by the Biotechnology and Biological Sciences Research Council grant BB/K016164/1 (Core Support for Collaborative Research to A.D. and S.M.H.), and by the Wellcome Trust (Senior Investigator Award to A.D.). This work was also supported in part by the NIH/NIEHS (P30-ES002109). A.S.D. was supported by the NIH/NIAMS (F31AR067615).

REFERENCES

Aebi M. N-linked protein glycosylation in the ER. Biochim Biophys Acta - Mol Cell Res. 2013; 1833:2430–2437.

Bagratuni T, Wu P, de Castro DG, Davenport EL, Dickens NJ, Walker BA, Boyd K, Johnson DC, Gregory W, Morgan GJ, et al. XBP1s levels are implicated in the biology and outcome of myeloma mediating different clinical outcomes to thalidomide-based treatments. Blood. 2010; 116:250–253. [PubMed: 20421453]

Batista BS, Eng WS, Pilobello KT, Hendricks-Munoz KD, Mahal LK. Identification of a conserved glycan signature for microvesicles. J Proteome Res. 2011; 10:4624–4633. [PubMed: 21859146]

Braakman I, Bulleid NJ. Protein folding and modification in the mammalian endoplasmic reticulum. Annu Rev Biochem. 2011; 80:71–99. [PubMed: 21495850]

Bull C, Stoel MA, den Brok MH, Adema GJ. Sialic acids sweeten a tumor's life. Cancer Res. 2014; 74:3199–3204. [PubMed: 24830719]

Campeau E, Ruhl VE, Rodier F, Smith CL, Rahmberg BL, Fuss JO, Campisi J, Yaswen P, Cooper PK, Kaufmann PD. A versatile viral system for expression and depletion of proteins in mammalian cells. PLoS One. 2009; 4:e6529. [PubMed: 19657394]

Caramelo JJ, Parodi AJ. Getting in and out from calnexin/calreticulin cycles. J Biol Chem. 2008; 283:10221–10225. [PubMed: 18303019]

Carrasco DR, Sukhdeo K, Protopopova M, Sinha R, Enos M, Carrasco DE, Zheng M, Mani M, Henderson J, Pinkus GS, et al. The differentiation and stress response factor XBP-1 drives multiple myeloma pathogenesis. Cancer Cell. 2007; 11:349–360. [PubMed: 17418411]

Ceroni A, Maass K, Geyer H, Geyer R, Dell A, Haslam SM. GlycoWorkbench: A tool for the computer-assisted annotation of mass spectra of glycans. J Proteome Res. 2008; 7:1650–1659. [PubMed: 18311910]

Chen MM, Bartlett AI, Nerenberg PS, Friel CT, Hackenberger CPR, Stultz CM, Radford SE, Imperiali B. Perturbing the folding energy landscape of the bacterial immunity protein Im7 by site-specific N-linked glycosylation. Proc Natl Acad Sci USA. 2010; 107:22528–22533. [PubMed: 21148421]

Chui D, Sellakumar G, Green R, Sutton-Smith M, McQuistan T, Marek K, Morris H, Dell A, Marth J. Genetic remodeling of protein glycosylation in vivo induces autoimmune disease. Proc Natl Acad Sci USA. 2001; 98:1142–1147. [PubMed: 11158608]

Culyba EK, Price JL, Hanson SR, Dhar A, Wong CH, Gruebele M, Powers ET, Kelly JW. Protein native-state stabilization by placing aromatic side chains in N-glycosylated reverse turns. Science. 2011; 331:571–575. [PubMed: 21292975]

de Leoz MLA, Young LJT, An HJ, Kronewitter SR, Kim JH, Miyamoto S, Borowsky AD, Chew HK, Lebrilla CB. High-mannose glycans are elevated during breast cancer progression. Mol Cell Prot. 2011; 10 M110.002717.

Dennis JW, Nabi IR, Demetriou M. Metabolism, cell surface organization, and disease. Cell. 2009; 139:1229–1241. [PubMed: 20064370]

Denzel MS, Storm NJ, Gutschmidt A, Baddi R, Hinze Y, Jarosch E, Sommer T, Hoppe T, Antebi A. Hexosamine pathway metabolites enhance protein quality control and prolong life. Cell. 2014; 156:1167–1178. [PubMed: 24630720]

East L, Isacke CM. The mannose receptor family. Biochim Biophys Acta. 2002; 1572:364–386. [PubMed: 12223280]

Elbein AD, Tropea JE, Mitchell M, Kaushal GP. Kifunensine, a potent inhibitor of the glycoprotein processing mannosidase I. J Biol Chem. 1990; 265:15599–15605. [PubMed: 2144287]

Elliott S, Lorenzini T, Asher S, Aoki K, Brankow D, Buck L, Busse L, Chang D, Fuller J, Grant J, et al. Enhancement of therapeutic protein in vivo activities through glycoengineering. Nature Biotechnol. 2003; 21:414–421. [PubMed: 12612588]

Fry SA, Afrough B, Lomax-Browne HJ, Timms JF, Velentzis LS, Leathem AJC. Lectin microarray profiling of metastatic breast cancers. Glycobiology. 2011; 21:1060–1070. [PubMed: 21507904]

Fujimoto T, Onda M, Nagai H, Nagahata T, Ogawa K, Emi M. Upregulation and overexpression of human X-box binding protein 1 (hXBP-1) gene in primary breast cancers. Breast Cancer. 2003; 10:301–306. [PubMed: 14634507]

Hammond C, Braakman I, Helenius A. Role of N-linked oligosaccharide recognition, glucose trimming, and calnexin in glycoprotein folding and quality-control. Proc Natl Acad Sci USA. 1994; 91:913–917. [PubMed: 8302866]

Hassinen A, Pujol FM, Kokkonen N, Pieters C, Kihlstrom M, Korhonen K, Kellokumpu S. Functional organization of Golgi N- and O-glycosylation pathways involves pH-dependent complex formation that is impaired in cancer cells. J Biol Chem. 2011; 286:38329–38340. [PubMed: 21911486]

Hauselmann I, Borsig L. Altered tumor-cell glycosylation promotes metastasis. Front Oncol. 2014; 4:28. [PubMed: 24592356]

Herscovics A. Importance of glycosidases in mammalian glycoprotein biosynthesis. Biochim Biophys Acta. 1999; 1473:96–107. [PubMed: 10580131]

Ioannou YA, Zeidner KM, Grace ME, Desnick RJ. Human alpha-galactosidase A: glycosylation site 3 is essential for enzyme solubility. Biochem J. 1998; 332:789–797. [PubMed: 9620884]

Iwamoto M, Björklund T, Lundberg C, Kirik D, Wandless TJ. A general chemical method to regulate protein stability in the mammalian central nervous system. Chem Biol. 2010; 17:981–988. [PubMed: 20851347]

Jacob GS, Scudder P. Glycosidases in structural analysis. Methods Enzymol. 1994; 230:280–299. [PubMed: 8139502]

Jang-Lee J, North SJ, Sutton-Smith M, Goldberg D, Panico M, Morris H, Haslam S, Dell A. Glycomic profiling of cells and tissues by mass spectrometry: Fingerprinting and sequencing methodologies. Glycobiology. 2006; 415:59–86.

Lau KS, Partridge EA, Grigorian A, Silvescu CI, Reinhold VN, Demetriou M, Dennis JW. Complex N-glycan number and degree of branching cooperate to regulate cell proliferation and differentiation. Cell. 2007; 129:123–134. [PubMed: 17418791]

Lee A-H, Iwakoshi NN, Glimcher LH. XBP-1 regulates a subset of endoplasmic reticulum resident chaperone genes in the unfolded protein response. Mol Cell Biol. 2003; 23:7448–7459. [PubMed: 14559994]

Lehle L, Tanner W. The specific site of tunicamycin inhibition in the formation of dolichol-bound N-acetylglucosamine derivatives. FEBS Lett. 1976; 72:167–170. [PubMed: 791682]

Moremen KW, Tiemeyer M, Nairn AV. Vertebrate protein glycosylation: diversity, synthesis and function. Nature Rev Mol Cell Biol. 2012; 13:448–462. [PubMed: 22722607]

Murray AN, Chen W, Antonopoulos A, Hanson SR, Wiseman RL, Dell A, Haslam SM, Powers DL, Powers ET, Kelly JW. Enhanced aromatic sequons increase oligosaccharyltransferase glycosylation efficiency and glycan homogeneity. Chem Biol. 2015; 22:1052–1062. [PubMed: 26190824]

Ron D, Walter P. Signal integration in the endoplasmic reticulum unfolded protein response. Nature Rev Mol Cell Biol. 2007; 8:519–529. [PubMed: 17565364]

Ruiz-Canada C, Kelleher DJ, Gilmore R. Cotranslational and posttranslational N-glycosylation of polypeptides by distinct mammalian OST isoforms. Cell. 2009; 136:272–283. [PubMed: 19167329]

Satoh T, Cowieson NP, Hakamata W, Ideo H, Fukushima K, Kurihara M, Kato R, Yamashita K, Wakatsuki S. Structural basis for recognition of high mannose type glycoproteins by mammalian transport lectin VIP36. J Biol Chem. 2007; 282:28246–28255. [PubMed: 17652092]

Schroder M, Kaufman RJ. The mammalian unfolded protein response. Annu Rev Biochem. 2005; 74:739–789. [PubMed: 15952902]

Sharon N. Lectins: Carbohydrate-specific reagents and biological recognition molecules. J Biol Chem. 2007; 282:2753–2764. [PubMed: 17145746]

Shoulders MD, Raines RT. Collagen structure and stability. Annu Rev Biochem. 2009; 78:929–958. [PubMed: 19344236]

Shoulders MD, Ryno LM, Cooley CB, Kelly JW, Wiseman RL. Broadly applicable methodology for the rapid and dosable small molecule-mediated regulation of transcription factors in human cells. J Am Chem Soc. 2013a; 135:8129–8132. [PubMed: 23682758]

Shoulders MD, Ryno LM, Genereux JC, Moresco JJ, Tu PG, Wu C, Yates JR 3rd, Su AI, Kelly JW, Wiseman RL. Stress-independent activation of XBP1s and/or ATF6 reveals three functionally diverse ER proteostasis environments. Cell Rep. 2013b; 3:1279–1292. [PubMed: 23583182]

Spear ED, Ng DTW. Single, context-specific glycans can target misfolded glycoproteins for ER-associated degradation. J Cell Biol. 2005; 169:73–82. [PubMed: 15809311]

Stowell SR, Ju T, Cummings RD. Protein glycosylation in cancer. Annu Rev Pathol. 2015; 10:473–510. [PubMed: 25621663]

Taylor RC, Dillin A. XBP-1 is a cell-nonautonomous regulator of stress resistance and longevity. Cell. 2013; 153:1435–1447. [PubMed: 23791175]

Thibault G, Ismail N, Ng DTW. The unfolded protein response supports cellular robustness as a broad-spectrum compensatory pathway. Proc Natl Acad Sci USA. 2011; 108:20597–20602. [PubMed: 22143797]

Tigges M, Fussenegger M. XBP1-based engineering of secretory capacity enhances the productivity of Chinese hamster ovary cells. Metabol Eng. 2006; 8:264–272.

Tulsiani DRP, Harris TM, Touster O. Swainsonine inhibits the biosynthesis of complex glycoproteins by inhibition of Golgi mannosidase II. J Biol Chem. 1982; 257:7936–7939. [PubMed: 6806288]

Venetz D, Hess C, Lin CW, Aebi M, Neri D. Glycosylation profiles determine extravasation and disease-targeting properties of armed antibodies. Proc Natl Acad Sci USA. 2015; 112:2000–2005. [PubMed: 25646460]

Voss M, Kunzel U, Higel F, Kuhn PH, Colombo A, Fukumori A, Haug-Kroper M, Klier B, Grammer G, Seidl A, et al. Shedding of glycan-modifying enzymes by signal peptide peptidase-like 3 (SPPL3) regulates cellular N-glycosylation. EMBO J. 2014; 33:2890–2905. [PubMed: 25354954]

Walter P, Ron D. The unfolded protein response: From stress pathway to homeostatic regulation. Science. 2011; 334:1081–1086. [PubMed: 22116877]

Wang ZV, Deng Y, Gao N, Pedrozo Z, Li DL, Morales CR, Criollo A, Luo X, Tan W, Jiang N, et al. Spliced X-box binding protein 1 couples the unfolded protein response to hexosamine biosynthetic pathway. Cell. 2014; 156:1179–1192. [PubMed: 24630721]

Wujek P, Kida E, Walus M, Wisniewski KE, Golabek AA. N-Glycosylation is crucial for folding, trafficking, and stability of human tripeptidyl-peptidase I. J Biol Chem. 2004; 279:12827–12839. [PubMed: 14702339]

Zielinska DF, Gnad F, Wisniewski JR, Mann M. Precision mapping of an in vivo N-glycoproteome reveals rigid topological and sequence constraints. Cell. 2010; 141:897–907. [PubMed: 20510933]

Highlights

- XBP1s regulates N-glycan maturation pathways, in addition to proteostasis
- XBP1s can enhance synthesis of hybrid and complex N-glycans on secreted proteins
- Regulating N-glycodynamics is a new function for the unfolded protein response
- XBP1s–mediated alterations in the N-glycome could have key biological impacts

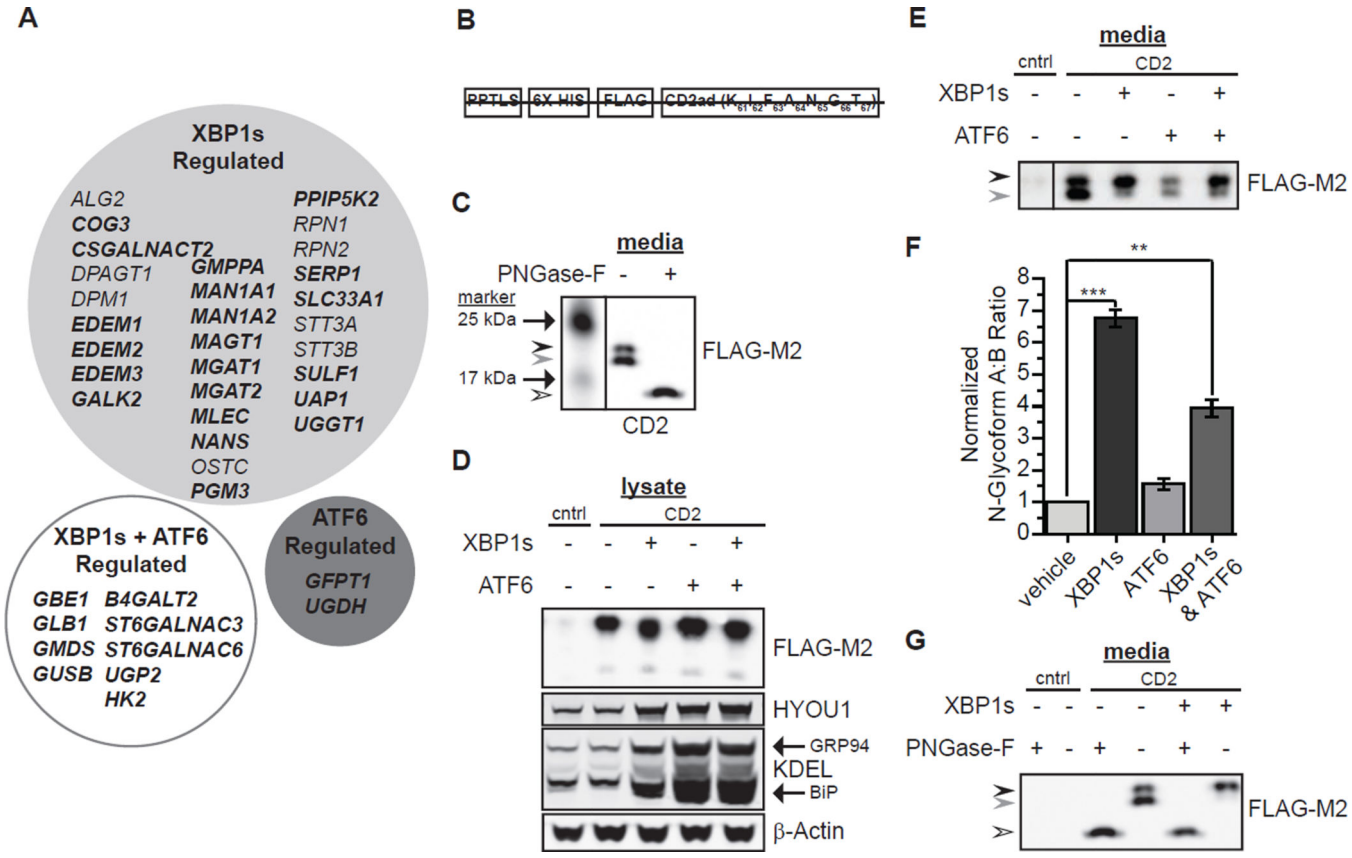

Figure 1. XBP1s Modulates the Molecular Architecture of CD2's N-Linked Glycan

(A) Gene ontology enrichment analysis identifies numerous genes involved in N-glycoprotein biosynthesis (regular italic typeface) and potentially in N-glycan maturation (bold italic typeface) that are upregulated primarily by XBP1s (light gray circle). In addition, a subset of N-glycosylation-related genes is induced primarily by ATF6 (dark gray circle) or only when both XBP1s and ATF6 are activated (white circle). *MGAT1* upregulation was identified by qPCR.

(B) The CD2 expression construct includes the preprotrypsin leader sequence (PPTLS), a 6X–His tag, a FLAG tag, and the single N-glycosylation sequon shown.

(C) Immunoblot of media harvested from HEK293 cells expressing CD2 displays two distinct bands; N-glycoforms A (black arrow) and N-glycoforms B (gray arrow). PNGase F digestion collapses both bands to a single lower molecular weight band (white arrow).

(D) Representative immunoblot of lysates from HEK293$^{DAX\text{-}CD2}$ cells after 72 h of XBP1s and/or ATF6 activation (Dox at 1 μg/mL and/or TMP at 10 μM). A single N-glycosylated band and a faint non-N-glycosylated band are observed. Probing for known UPR-upregulated proteins confirms transcription factor activation.

(E) Representative immunoblot of CD2 in media corresponding to the lysate samples in **Figure 1D**. Control media is from parent HEK293^{DAX} cells.

(F) Quantification of the data in **Figure 1E**. Error bars represent SEM from biological replicates (n = 3). $^{**}p < 0.005$, $^{***}p < 0.0005$.

(G) Immunoblot showing PNGase digestion of CD2 secreted from HEK293$^{DAX\text{-}CD2}$ cells. See also Table S1 and Figure S1.

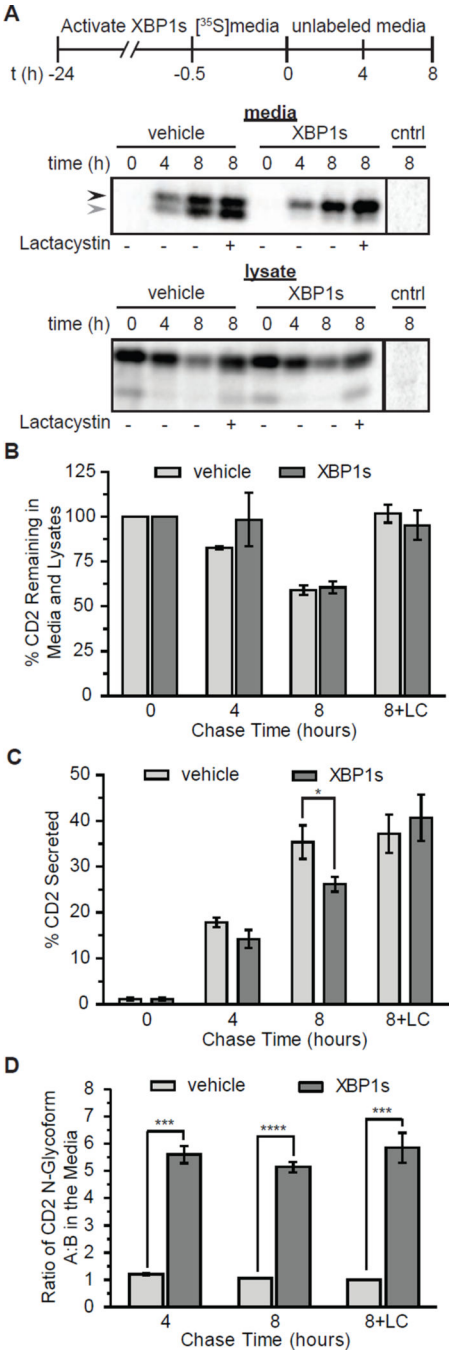

Figure 2. XBP1s Activation Does Not Significantly Influence CD2 Secretion or Degradation

(A) Representative autoradiograms of [^{35}S]-labelled CD2 immunoisolated from HEK293$^{DAX\text{-}CD2}$ media and lysates following a 24 h pre-activation of XBP1s (Dox; 1 μg/mL) or no treatment. The metabolic labeling protocol employed is shown. Control media and lysate were harvested from parent HEK293^{DAX} cells. Lactacystin (LC) inhibits proteasomal degradation of CD2.

(B–D) Quantification of autoradiograms in **Figure 2A**. % CD2 remaining in **Figure 2B** was calculated by normalizing the secreted and lysate CD2 signal at the stated times to the total

amount of labeled CD2 observed at time = 0 h. % CD2 secreted in **Figure 2C** was calculated by normalizing the secreted CD2 signal to the total amount of CD2 present at time = 0 h. The N-glycoforms ratio A:B in **Figure 2D** was calculated as in Figure 1F. Error bars represent SEM from biological replicates (n = 3). *$p < 0.05$, ***$p < 0.005$, ****$p < 0.001$.

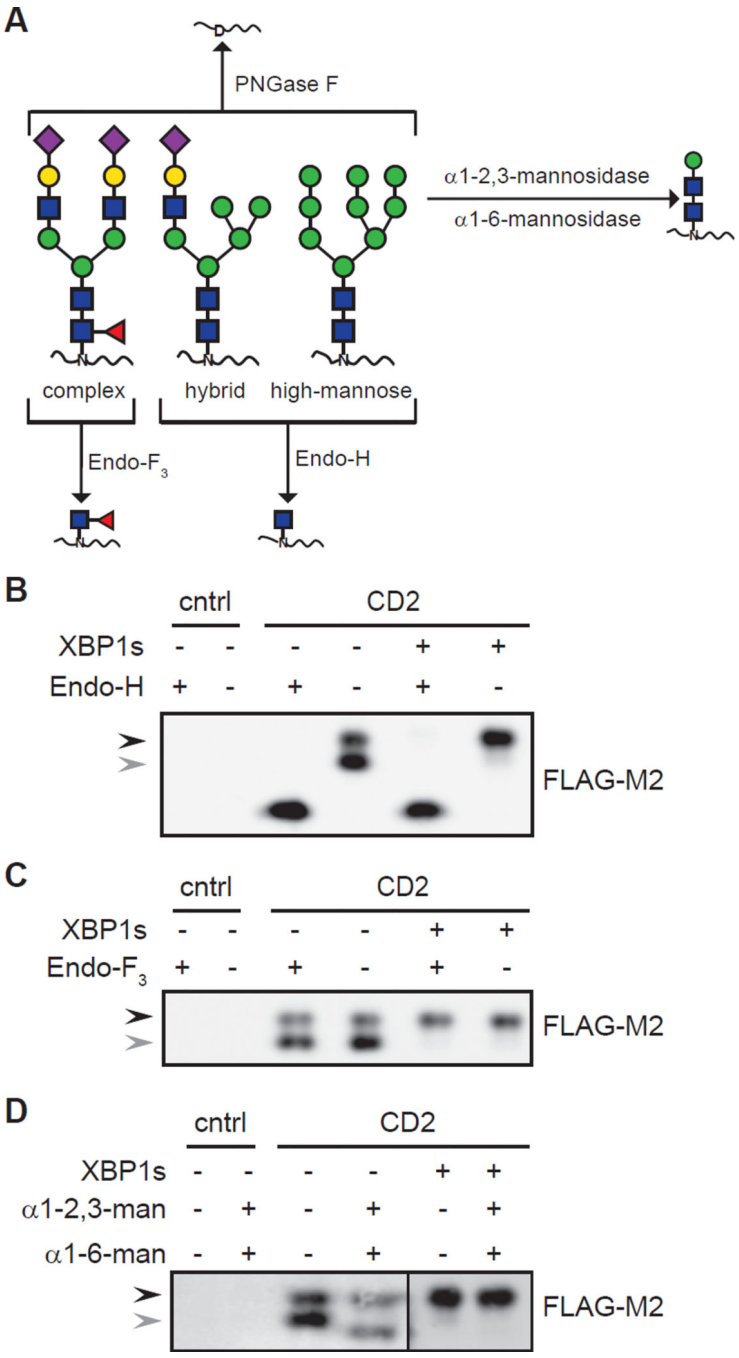

Figure 3. Glycosidase Digestions to Characterize N-Glycans on Secreted CD2

(A) Schematic displaying cleavage patterns of N-glycans by endo and exo-glycosidases. Color symbols are: purple diamond, N-acetylneuraminic acid; blue square, N-acetylglucosamine; green circle, mannose; red triangle, fucose.

(B–D) Immunoblots of CD2 secreted from either untreated or XBP1s-activated HEK293$^{DAX\text{-}CD2}$ cells as in Figure 1E and digested with the indicated glycosidases. Endo-H cleaves both N-glycoforms A and B indicated by the blue and green arrows, yielding the mono-GlcNAcylated product indicated by the orange arrow (**Figure 3B**). Endo-F_3 does not

significantly cleave either N-glycoform band (**Figure 3C**). Double digestion by the α1–2,3- and α1–6-mannosidases reduces only the molecular weight of N-glycoforms B (**Figure 3D**).

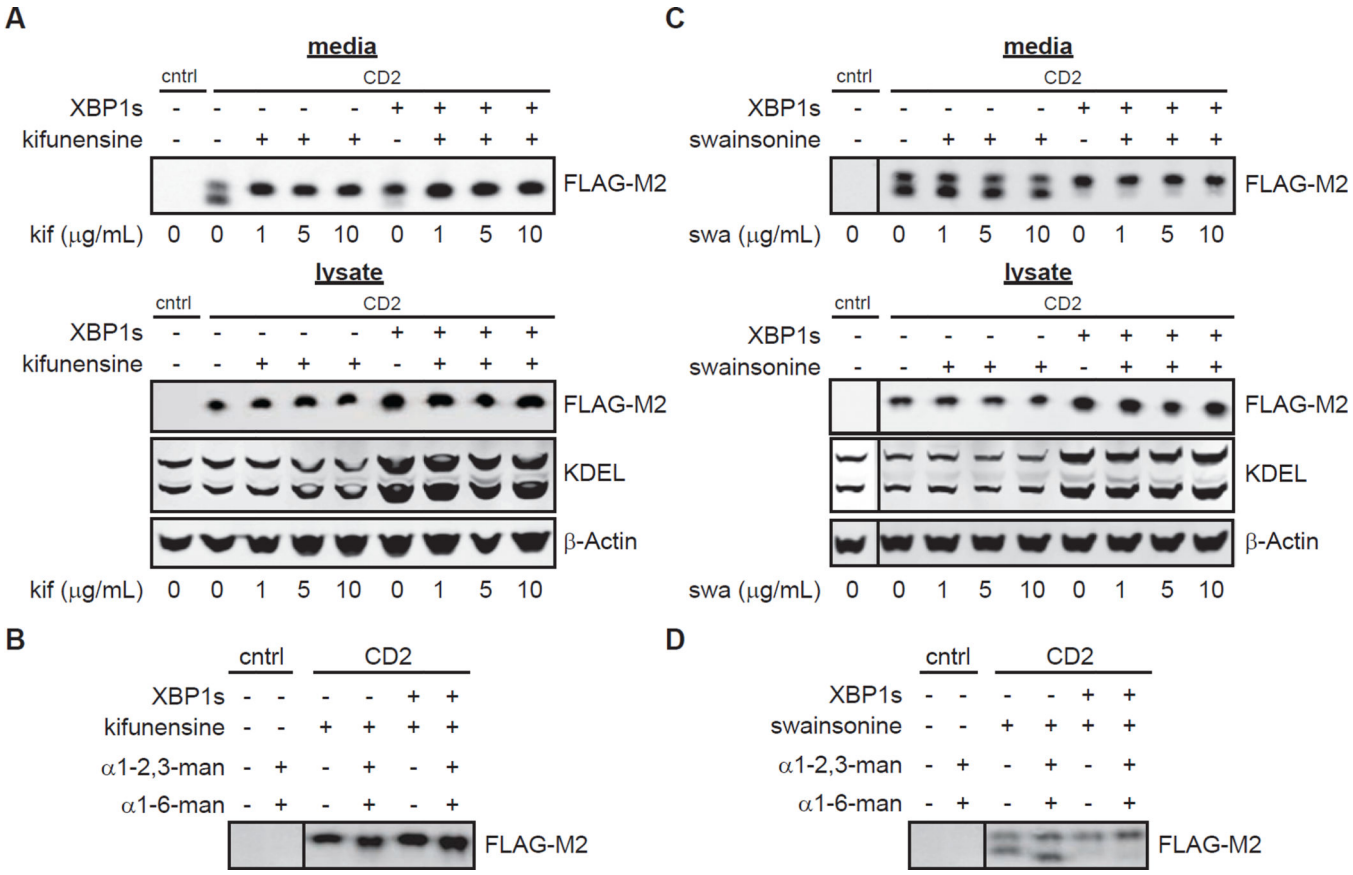

Figure 4. Effects of XBP1s Activation Upon Inhibition of α-Mannosidase-I or -II

Immunoblots are of CD2 secreted from untreated or XBP1s-activated HEK293$^{DAX\text{-}CD2}$ cells as in Figure 1E.

(A) Preventing formation of both hybrid and complex N-glycans by inhibiting α-mannosidase-I with kifunensine (kif) eliminates the effects of XBP1s activation on CD2 N-glycan maturation.

(B) Double digestion by the α1–2,3 -and α1–6-mannosidases reduces the molecular weight of secreted CD2 from **Figure 4A**, confirming it is a high mannose N-glycoform.

(C) Preventing formation of complex N-glycans by inhibiting α-mannosidase-II with swainsonine (swa) has no observable impact on the effects of XBP1s activation on CD2 N-glycan biosynthesis.

(D) Double digestion by the α1–2,3- and α1–6-mannosidases only influences the molecular weight of N-glycoforms band B from non-XBP1s-activated HEK293$^{DAX\text{-}CD2}$ cells treated with swainsonine in **Figure 4C**.

See also Figure S2.

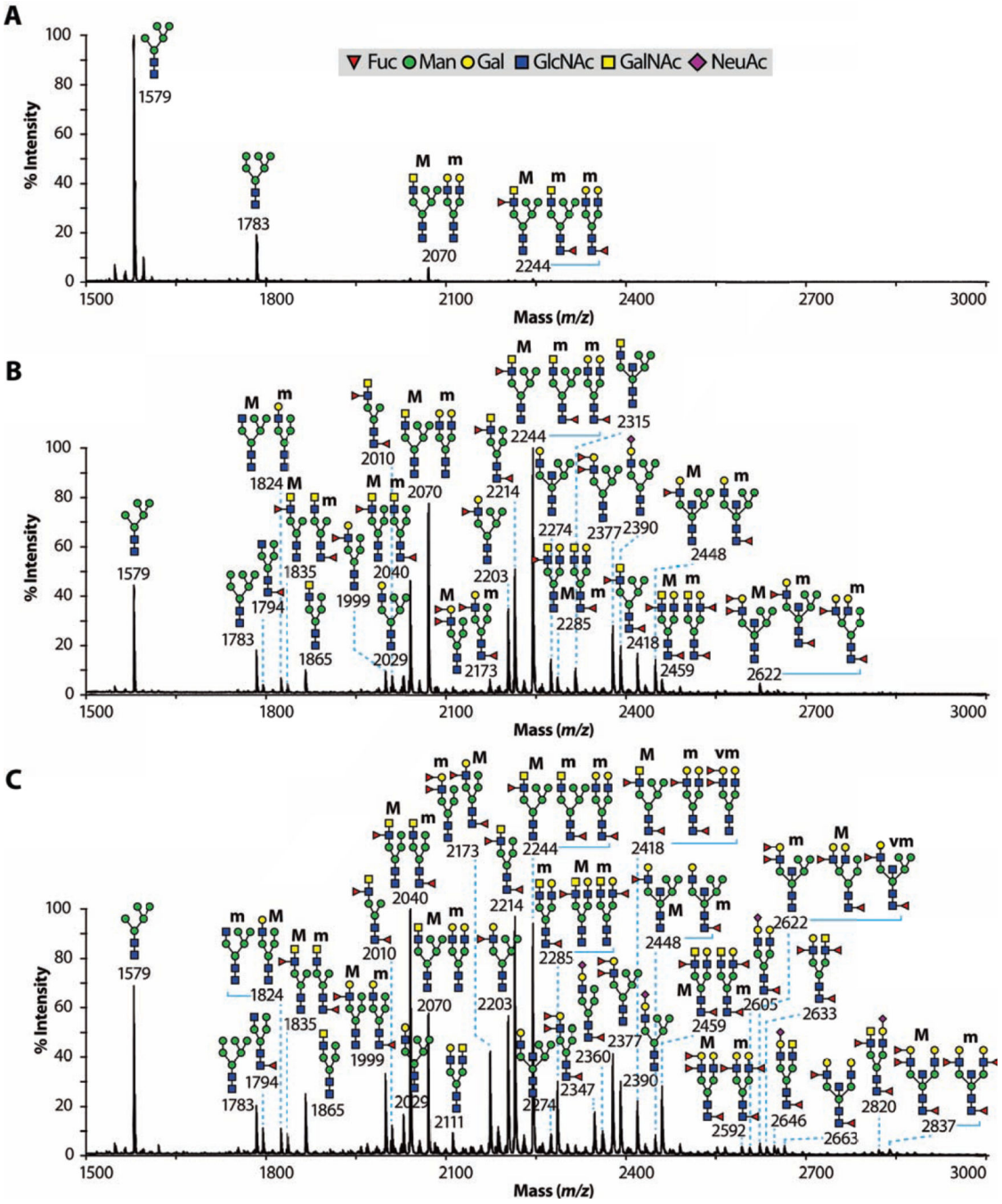

Figure 5. Mass Spectrometry-Based Glycomic Analyses Reveal the Molecular Structures of CD2 N-Glycans Upon XBP1s Activation

MALDI-TOF mass spectra of permethylated N-glycans released by PNGase F digestion of CD2 purified from the media of untreated or XBP1s-activated HEK293$^{DAX\text{-}CD2}$ cells. In untreated cells, N-glycoforms bands A (**Figure 5A**) and B (**Figure 5B**) were analyzed separately. In XBP1s-activated cells, the bands were analysed together (**Figure 5C**).

(A) N-Glycoforms band B for CD2 secreted from untreated cells is homogenous and high mannose.

(B) N-Glycoforms band A for CD2 secreted from untreated cells is primarily hybrid.
(C) For CD2 from XBP1s-activated cells, N-glycoforms bands A and B were analyzed together. Hybrid and complex N-glycans are much more prominent in the XBP1s-activated sample than in the vehicle-treated sample (e.g., *m/z* 1999, 2040, 2173, 2214, 2347 and 2360 for hybrid structures and *m/z* 2211, 2285, 2418, 2459, 2592, 2605, 2633, 2646, 2820, 2837 for complex structures), a difference whose magnitude is illustrated by normalizing to the relative intensities of bands A and B from vehicle-treated cells. Differences are also noted in the terminal N-glycan epitopes relative to untreated cells. These quantitations are presented in Table 1.
Color symbols are: yellow square, N-acetylgalactosamine; blue square, N-acetylglucosamine; yellow circle, galactose; green circle, mannose; purple diamond, N-acetylneuraminic acid; red triangle, fucose. All molecular ions are $[M + Na]^+$. Putative structures are based on composition, tandem MS, and biosynthetic knowledge. Structures that show sugars outside a bracket have not been unequivocally defined. Letters “m” and “M” in bold characters suggest minor and major abundances respectively.
See also Figure S3.

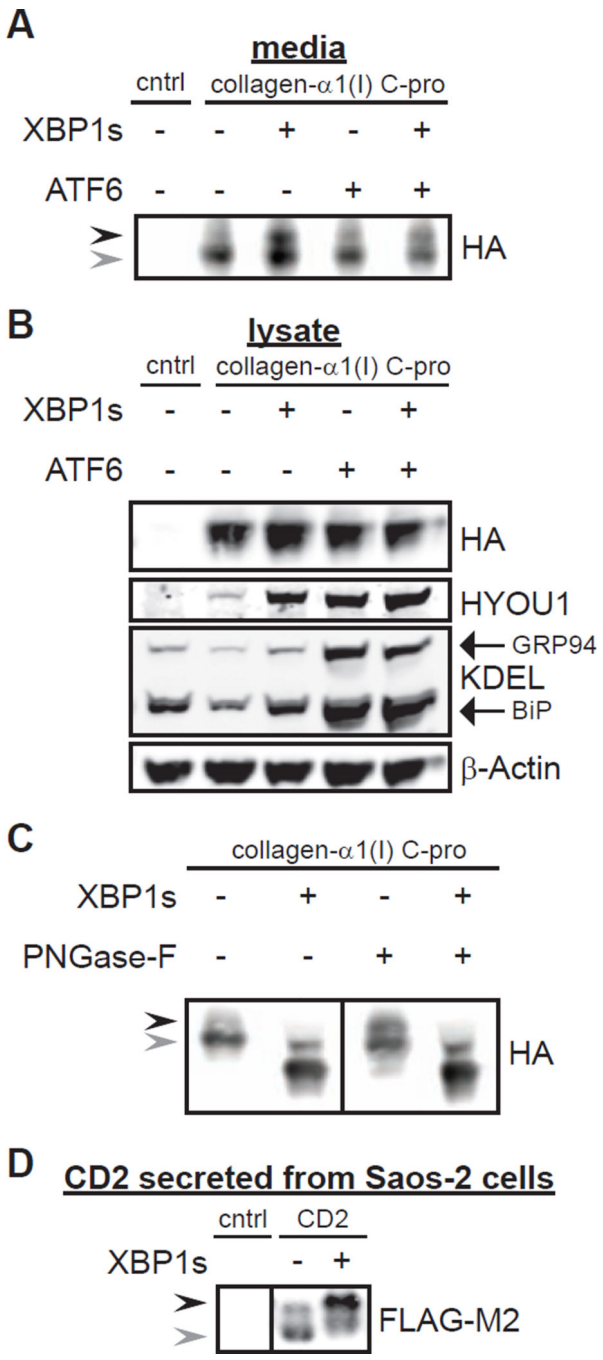

Figure 6. XBP1s Activation Modulates the Molecular Architecture of Mature N-Glycans on the Collagen-α1(I) C-Propeptide and in Saos-2 Cells

(A) Representative immunoblot of the collagen-α1(I) C-propeptide in media collected from HEK293^{DAX} cells stably expressing the protein after 48 h of stress-independent XBP1s and/or ATF6 activation (Dox at 1 μg/mL and/or TMP at 10 μM). Two N-glycoforms bands A and B are observed, as indicated by the arrows. XBP1s activation enhances levels of the top band. Control media was harvested from parent HEK293^{DAX} cells.

(B) Representative immunoblot of lysates corresponding to the media samples in **Figure 6A**.

(C) Immunoblot showing PNGase digestion of collagen-α1(I) C-propeptide samples secreted from untreated and XBP1s-activated HEK293^{DAX} cells as in **Figure 6A**.
(D) Immunoblot of CD2 secreted over 48 h from transiently transfected Saos-2 cells co-transduced with either a GFP-encoding or an XBP1s–encoding adenovirus. Samples for analysis were obtained via a FLAG-M2-mediated immunoprecipitation of CD2 from the media. Two N-glycoforms bands A and B are observed, as indicated by the arrows. XBP1s activation enhances levels of the top band. Control media was harvested from GFP-transfected Saos-2 cells.
See also Figure S4.

Table 1

Summary of MALDI-TOF-MS/MS glycomic analyses of CD2.

N-Glycan Classification		
type	**vehicle (%)**	**XBP1s (%)**
complex	5	16
hybrid	35	74
high-mannose	61	11
N-Glycan Terminal Epitope[a]		
epitope	vehicle (%)	XBP1s(%)
LacdiNAc	29	19
Fuc-LacdiNAc	47	39
LacNAc	10	15
LeX/A (Lewis X/A)[b]	4	10
LeY/B (Lewis Y/A)[b]	7	11
S-LacNAc[c]	4	6

[a] LacNAc, N-acetyllactosamine; LacdiNAc, N,N'-diacetyllactosamine; Fuc-LacdiNAc, Fucosylated LacNAc; S-LacNAc, Sialylated LacNAc.

[b] Lewis glycan epitope types.

[c] Sialylated LacdiNAc not detected.